The Synthesis and Characterization of Gold-Core/LDH-Shell Nanoparticles

by

Colton Rearick

A Thesis Presented in Partial Fulfillment
of the Requirements for the Degree
Master of Science

Approved April 2011 by the
Graduate Supervisory Committee:

Sandwip Dey, Chair
Stephen Krause
B Ramakrishna

ARIZONA STATE UNIVERSITY

May 2011

ABSTRACT

In recent years, the field of nanomedicine has progressed at an astonishing rate, particularly with respect to applications in cancer treatment and molecular imaging. Although organic systems have been the frontrunners, inorganic systems have also begun to show promise, especially those based upon silica and magnetic nanoparticles (NPs). Many of these systems are being designed for simultaneous therapeutic and diagnostic capabilities, thus coining the term, theranostics.

A unique class of inorganic systems that shows great promise as theranostics is that of layered double hydroxides (LDH). By synthesis of a core/shell structures, e.g. a gold nanoparticle (NP) core and LDH shell, the multifunctional theranostic may be developed without a drastic increase in the structural complexity.

To demonstrate initial proof-of-concept of a potential (inorganic) theranostic platform, a Au-core/LDH-shell nanovector has been synthesized and characterized. The LDH shell was heterogeneously nucleated and grown on the surface of silica coated gold NPs via a coprecipitation method. Polyethylene glycol (PEG) was introduced in the initial synthesis steps to improve crystallinity and colloidal stability. Additionally, during synthesis, fluorescein isothiocyanate (FITC) was intercalated into the interlayer spacing of the LDH. In contrast to the PEG stabilization, a post synthesis citric acid treatment was used as a method to control the size and short-term stability. The heterogeneous core-shell system was characterized with scanning electron microscopy (SEM), energy dispersive x-ray spectroscopy (EDX), dynamic light scattering (DLS), and powder x-ray diffraction (PXRD). A preliminary *in vitro* study carried out with the assistance of

Dr. Kaushal Rege's group at Arizona State University was to demonstrate the endocytosis capability of homogeneously-grown LDH NPs.

The DLS measurements of the core-shell NPs indicated an average particle size of 212nm. The PXRD analysis showed that PEG greatly improved the crystallinity of the system while simultaneously preventing aggregation of the NPs. The preliminary *in vitro* fluorescence microscopy revealed a moderate uptake of homogeneous LDH NPs into the cells.

ACKNOWLEDGMENTS

I would like to thank my advisor Dr. Sandwip Dey, Professor, School for Engineering of Matter, Transport and Energy, Arizona State University who has guided and supported me throughout my entire Master's program. Without him, I would not have had this amazing opportunity to learn and grow the way I have over the past two years of my graduate career. The enthusiasm and dedication he puts into everything he does both at and away from the university setting has truly been an inspiration. I extend my most sincere gratitude to Dr. Dey for this invaluable opportunity.

Thank you to Dr. Stephen Krause and Dr. B. Ramakrishna, School for Engineering of Matter, Transport and Energy, Arizona State University accepting positions on my M.S. thesis committee. I would also like to thank Dr. Robert Marzke, Professor, Department of Physics, Arizona State University for his support and guidance.

Thank you to Dr. Kaushal Rege, Assistant Professor, Arizona State University, and your student Jimmy Ramos for their cooperation on our research project. I extend my gratitude to Dr. Zhenquan Liu, and David Wright, LeRoy Eyring Center for Solid State Science, and Dr. Thomas Groy, Department of Chemistry and Biochemistry, Arizona State University for their assistance throughout my research.

Lastly, I would like to thank all of my colleagues in Dr. Dey's lab, Annette Hyla, Maneet Kamboj, Armando Licon, and especially Xiaodi Sun, with whom I worked side by side over the past 18 months. Special thanks to Kiril Hristovski from Dr. Westerhoff's lab for allowing us to spend countless hours on the Zeta potential and particle measurement unit.

I would like to acknowledge financial assistance from the National Science Foundation, Woman and Philanthropy, and the National Institute of Health-National Cancer Institute.

My final and most sincere thanks go to my parents. Without their support and encouragement, none of this would have been possible. Thank you.

TABLE OF CONTENTS

LIST OF TABLES

Table Page

LIST OF FIGURES

CHAPTER 1

INTRODUCTION

The treatment of cancer has always been a substantial undertaking. To date, the most common treatment options include chemotherapy, radiation therapy, and a select number of therapeutic drugs. In certain cases, each of these methods can be moderately effective, either slowing the progression or, ideally, forcing the cancer into remission. No matter the success, however, the fact remains that systemic cancer therapy is extremely invasive. Hair loss, weakness, body aches, nausea are all common side effects experienced by patients undergoing treatment for various cancers. These side effects of treatment can absolutely destroy the patient, both physiologically and mentally. Since the patient's immune system is generally completely compromised, a second treatment is required to boost the immune system and prevent further disease and side effects. It is obvious there is a need for alternative but targeted treatment method which is equally, or ideally, more effective while drastically reducing the strain on the patient.

This need has been the cause for intense research on the development of nanoparticle drug delivery platforms. A successful platform will combine the diagnostic and therapeutic capabilities of current technologies into one system, i.e., a theranostic. Many systems have been developed to date, and some polymeric platforms have already gained Food and Drug Administration (FDA) approval (Farokhzad and Langer). However, inorganic systems and specifically, layered double hydroxides (LDH) have begun to exhibit high potential for their unique ability to be intercalated with anionic species.

Discovered in the nineteenth century, LDHs have attracted increasing attention for their potential applications in catalysis, adsorption, and drug delivery. Naturally occurring LDHs are found in the rhombohedral and hexagonal polymorphic forms with the hexagonal structure providing greater interlayer spacing for intercalation various species. Specific LDHs such as (Mg, Al), (Zn, Al), (Li, Al), and (Mg, Fe) can be used for a drug delivery platform because of their physiochemical properties and biocompatibility. LDH is favored for its ability to reduce drug toxicity and side effects, lower dosage, and increase drug potency (Dey and Sistiabudi). More specifically, LDH is a structurally new family of anionic clays that consist of cationic brucite like layers and exchangeable interlayer anions. In Figure 1, the positively charged layers are seen as gray octahedra and the intercalated anions are represented by the green spheres (Dey and Sistiabudi). The LDH compositions are commonly represented by the formula $[M^{z+}_{1-x}M^{3+}_{x}(OH)_2]^{q+}(X^{n-})_{q/n}\bullet yH_2O$ where y is a real number. In most instances, z = 2, and M^{2+} = Ca^{2+}, Mg^{2+}, Mn^{2+}, Fe^{2+}, Co^{2+}, Ni^{2+}, Cu^{2+} or Zn^{2+}; hence q = x. Despite having the existence of pure phases over the range $0.15 \leq x \leq 0.4$, values of x exist usually in the range $0.1 \leq x \leq 0.5$. It is also possible to have z = 1, where M^{+} = Li^{+} and M^{3+} = Al^{3+} thus resulting q = 2x - 1

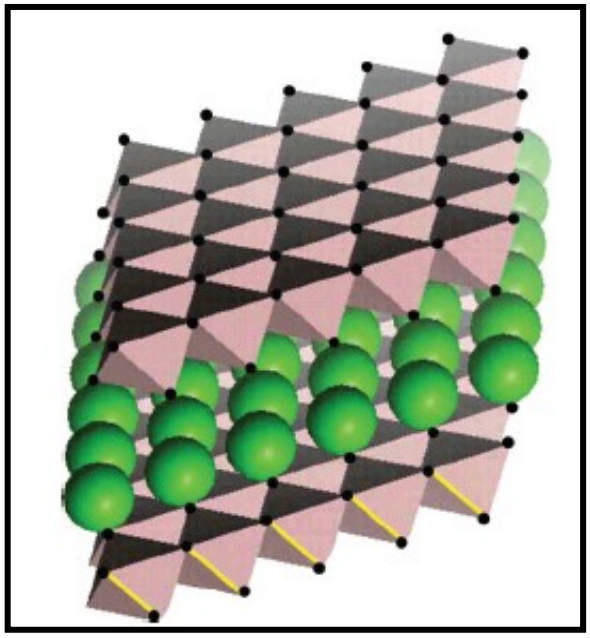

Figure 1 - Crystal structure of LDH

(Choy, Jung, et al.; Dey and Sistiabudi). The cations used in LDH are M^{2+} and M^{3+} ions such as Mg^{2+}, Zn^{2+} and Al^{3+}, Fe^{3+}, Gd^{3+} respectively. The layers of metal cations of similar ionic radii are coordinated by six oxygen atoms forming $M^{2+}/M^{3+}(OH)_6$ octahedra, which are 2-D sheets formed by edge sharing and stacked together by hydrogen bonding between the hydroxyl groups of adjacent sheets. Due to the high positive charge in the LDH structure (Carlino), anions must be intercalated between the adjacent cationic layers to maintain neutrality. The interlayer region is a fluid space containing water molecules, which are connected to both the metal hydroxide and interlayer anions through strong hydrogen bonding. A schematic of the above described structure can be seen in Figure 2. In this figure, carbonate anions are intercalated, maintaining charge neutrality, however, as stated, various species can be incorporated.

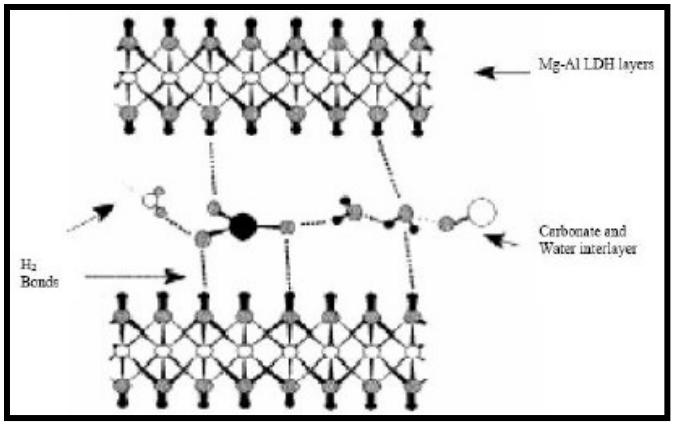

Figure 2 - - Interlayer stacking of carbonate ions and water molecules in (Mg, Al) LDH

These structural characteristics allow various dyes and therapeutic drugs to be incorporated into surface-functionalized LDH structures: to be within a biological system with site specificity. Within the LDH structure, the intercalated agent is prevented from interacting with surroundings until the targeted site is reached and penetrated, potentially minimizing any side effects, and providing a method for a precisely controlled release platform. Moreover, LDH can combined into a core-shell system, producing a theranostic nanovector which

contains multiple treatment options. By designing such a system, the favorable properties of LDH remain unchanged, while the system as a whole gains additional therapeutic and diagnostic modalities.

Therefore, the purpose of this research is the initial proof-of-concept of a multi modal theranostic core-shell nanoparticle system, specifically a Au-core/LDH-shell nanovector. Although LDH nanoparticles have been extensively studied, the incorporation of LDH into a core-shell system remains uncharted territory. The current research will include controllable size and size distribution, high colloidal stability, intercalation with an appropriate anionic dye, and initial *in vitro* imaging.

The intellectual merit of this work lies in the innovative improvement to current cancer diagnosis and treatment options through the use of nanomedicine. By combining two dissimilar materials (i.e., gold and LDH) into a core-shell structure, the unique properties of each may be exploited to produce a multi modal nanoparticle theranostic . The successful synthesis of this nanoparticle system will include intense experimentation and material characterization and will lead to *in vitro* and *in vivo* studies on various cancers. Although the development of the nanoparticle system within this work is primarily focused on the diagnosis and treatment of cancer, the broader impact will be the passage of nanomedicine onto the treatment of other diseases. The theranostic properties of this multi modal system fulfill the need for an improvement on the early detection and suppression of cancer and place this platform alongside the polymeric and quantum dot platforms which have already been developed.

Dynamic Light Scattering

A brief introduction to the technique of dynamic light scattering (DLS) is necessary for a better understanding results within. DLS is a characterization technique commonly used to measure particle size and size distribution. Small particles in suspension experience Brownian motion, causing the particles to rotate and change position constantly. The DLS technique measures this motion and then translates to a particle size.

A monochromatic light source (~635 nm) is incident on the suspension. Upon interacting with the particles, the light is scattered in all directions and then measured by a photomultiplier tube. Due to the constant motion of the particles, the measured intensity varies randomly with time. An autocorrelation function is then computed in order to derive the diffusion constant, which is further used to compute the particle size.

The autocorrelation function: $C(\tau) = Ae^{-2Dtq^2} + B$, where A and B are instrument constants, D is the diffusion constant, t is time, and q is the scattering vector, produces an exponential decay, an example of which can be seen in Figure 3 (Brookhaven Instruments Corporation). The time (x-axis) at which the decay begins corresponds to the particle size. Smaller particles move more quickly, causing the intensity to fluctuate more rapidly leading to decay in the correlation

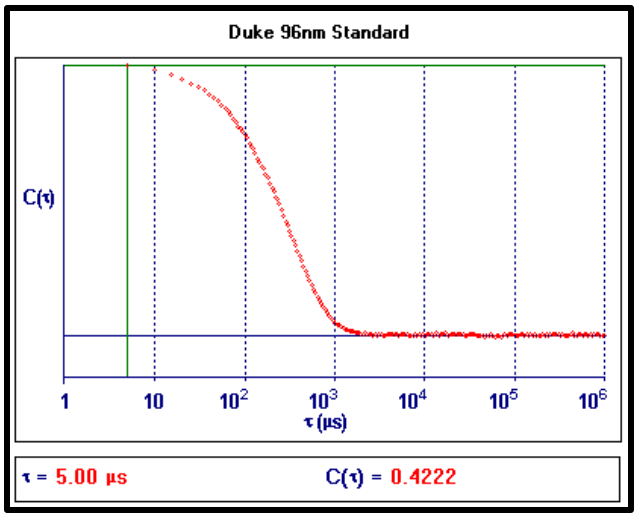

Figure 3 - Example of autocorrelation function for monodisperse suspension

function at a smaller time interval. The opposite is true of larger particles. Also notice the smooth, uniform decay, a characteristic of a monodisperse size distribution. As the polydispersity of the suspension increases, secondary humps in the curve begin to form, indicating multiple size distributions. Examples of various correlation functions are shown in the results and discussion section.

CHAPTER 2

LITERATURE REVIEW

Structure and Synthesis Layered Double Hydroxides (LDH)

The synthesis of layered double hydroxides (LDH) has been confined to three methods: an increasing pH method, where the pH of the precipitation reaction begins at a low value and is systematically increased through the solubility limits of both the divalent and trivalent metal ions; a constant pH low supersaturation method, in which the pH is started and maintained at a level just slightly above the trivalent ion; and a constant pH high supersaturation method, where the pH is started and maintained at a saturation value well above the M^{3+} ion. As the overall purity, size, and morphology is strongly dependent on the synthesis conditions, each of the above methods has been found to produce vastly different results.

With the increasing pH method, the precipitation of LDH occurs in two steps. First, the least soluble metal oxide, generally $M^{3+}(OH)_3$, is precipitated out of solution when the pH passes the solubility limit. As the pH is further increased, the more soluble divalent metal hydroxide precipitates, facilitating the formation of LDH (Dey and Sistiabudi). In titration curve, each of the precipitations corresponds to a plateau in the curve. It has been reported, that the pH at which each of the hydroxides precipitates is dependent on the relative stabilities of each individual species. Specifically, a lower solubility of a given $M^{2+}(OH)_2$ leads to a lower pH required for the formation of LDH. Conversely, a lower solubility of a given $M^{3+}(OH)_3$ translates to LDH formation at a higher pH (Boclair and Braterman); (Dey and Sistiabudi). This is expected because $M^{3+}(OH)_3$ is precipitated first, and is thus a reactant in the final LDH structure. It

is known that LDH can be formed with several divalent (Mg^{2+}, Zn^{2+}) and trivalent (Al^{3+}, Fe^{3+}, Cr^{3+}) metals, thus the precise pH values of precipitation vary. As reported by Dey et al., the titration plateaus of the commonly formed (Mg,Fe), (Zn,Fe), and (Mg,Al) LDH occur at a pH of (2.2, 8.3), (4.0, 7.6), and (2.3, 6.3), respectively. These values are, however, are highly dependent on solvent, concentration, temperature, and other controllable experimental parameters.

A special note must be given to $Fe(OH)_3$ for the synthesis of Fe-based LDH. Several studies have reported a rapid polymerization of $Fe(OH)_3$ at low to moderate pH ranges (Sato et al.); (Meng et al.); (Boclair and Braterman). When this occurs, the Fe^{3+} in the system may be completely depleted, and as it is a necessary reactant in the precipitation of the $M^{2+}(OH)_2$ and formation of LDH, the reaction comes to a stand-still and LDH is not formed. Because of this, the increasing pH method, specifically for the formation of Fe containing LDH, is rendered useless and other precipitation techniques should be used.

The constant pH method, both under low and high supersaturation conditions, has generally had more success for the formation of LDH. The degree of supersaturation is not equally effective for all classes of LDH. Instead, the pH must be carefully chosen depending on the constituents of the LDH which is desired. (Mg,Al) LDH, has been successfully synthesized in both low and high supersaturation conditions, however the resulting particle size is affected by the reaction parameters (Choy, Jung, et al.); (Boclair and Braterman);(Dey and Sistiabudi). The same is not true with the (Mg,Fe) and (Zn,Fe) LDH systems. When forming (Mg,Fe) LDH, again, care must be taken to avoid the polymerization of $Fe(OH)_3$. To prevent this, it is most suitable to use the high supersaturation method, with the pH maintained at or above 12 (Sato et al.)

(Reichle). At this pH, both $Mg(OH)_2$ and $Fe(OH)_3$ precipitate rapidly and LDH is formed with relative ease.

In the case of (Zn,Fe) LDH, the high supersaturation method leads to problems with the formation of LDH. At a pH above 12, $Zn(OH)_2$is found to partially dehydrate, forming ZnO (Boclair and Braterman); (Meng et al.). Alternatively, the pH may be maintained slightly below 12, or the increasing pH method may be used. In both situations, the polymerization of Fe^{3+} occurs and the formation of crystalline LDH is not observed (Dey and Sistiabudi). It seems that (Zn,Fe) LDH may only formed via the low supersaturation method, maintaining the pH between 7-9. In this range, however, the precipitation of both hydroxides is expected to occur more slowly, which may lead to a larger particle size with lower crystallinity.

Nanomedicine

In recent decades, research on nanomedicine has opened the door for novel nanoparticle-based systems which may be used for imaging and treatment of diseases. Polymeric and inorganic systems provide an opportunity to improve upon the current technologies available for diagnosis and treatment of diseases. This task, however, is a non-trivial one. The size distribution and structure of these systems must be precisely controlled to achieve the desired properties. Additionally, the toxicity of nanoparticles must be closely studied to ensure safety and biocompatibility. At this point, nanomaterials have been largely centered around polymeric and nucleic acid based platforms (Farokhzad and Langer; Brannon-Peppas and Blanchette; Moghimi and Kissel). More recently, however, quantum dots (QDs) and core-shell platforms have taken center stage. These platforms not only enhance the capabilities of current nanomedicine, but also

broaden the diagnosis and treatment options that have otherwise been unachievable.

Fluorescent biomolecules are an important tool when investigating many of the basic structural properties of biological structures. They are capable of detecting and precisely locating minute, physiologically-relevant structures within biological systems. The most common fluorescent species used are organic molecules, proteins, metal chelators, and bioluminescent agents (Chaves et al.). Each of these species, however, have distinct disadvantages, i.e., low brightness, photobleaching, and high toxicity. The issue of emission brightness may be overcome by increasing the dose, however, this compounds to higher toxicity, making this an unsuitable option (Bardhan, Grady and Halas). Quantum dots are now being investigated to circumvent theses problems. Quantum dots first appeared for biological applications in 1998 (Chan and Nie; Bruchez et al.). Chan et al. designed detection labels by combining luminescent CdSe QDs with biological molecules. The CdSe QDs were capped with a layer of ZnS and then conjugated with targeting biomolecules, producing a system with luminescent quantum yield as high as 50% and emission wavelengths be controlled by tuning the particle size. Additionally, the nanohybrids were found to be biocompatible with very low toxicity (Chan and Nie). However, as is the case with many developing nanosystems, controlling the polydispersity of the QDs remains an issue.

More recently, core-shell nanostructures are being developed for biological applications. The core materials most often consist of noble metal nanoparticles (for their unique optical properties and biointertness), QDs (luminescent properties), silica, and magnetic and superparamagnetic

nanoparticles (imaging). The shell materials are also numerous, including: organic molecules such as thiols, fullerenes, and polyethylene glycol (PEG), silica, noble metals, and organic dyes. The most obvious advantage of core-shell nanostructures is the enhancement of the beneficial properties of the individual components when combined into hybrid structures. Additionally, by containing chemicals which are normally toxic within biocompatible shells, the desired properties can still be obtained without creating a health risk.

As discussed, many organic dyes, specifically near-infrared (NIR) emitting dyes, are toxic in relatively low quantities and produce mediocre quantum yields, at best. However, by incorporating these fluorescent molecules into core-shell structures, the quantum yield can be drastically improved and the toxicity issue all but eliminated. Bardhan et al. proposed a method to enhance the fluorescence of NIR emitting molecules by combining them with "metallic antennas." A core-shell system was developed containing a gold nanoparticle core (166 nm to 236 nm $\pm$ 4nm) with a thin silica shell of varying thickness (Bardhan, Grady and Halas). The silica shell provides an excellent platform for the absorption of organic dyes and also prevents the formation of free radicals within biological systems, rendering them biocompatible. The surface plasmon properties of the metal core enhances the fluorophores emission properties by decreasing the radiative lifetime (Bardhan, Grady and Halas; Chance, Prock and Silbey).

Intercalation of LDH and *In vitro* and *In vivo* Studies

As the field of nanomedicine has rapidly progressed with targeted drug delivery platforms at the front of the pack, a great amount of interest has been focused on LDH as a passive, controlled release, drug delivery platform (Dey and Sistiabudi; Del Arco et al.; Kwak et al.; Wei et al.; Tyner, Schiffman and Giannelis; Tronto et al.). Since the anions in the interlayer region are replaceable, a wide variety of species can take their place under controlled conditions in a process known as intercalation. There is evidence that many important bio-molecular agents have been intercalated inside the (Mg^{2+}, Al^{3+}) LDH structure including glycerol, organic acids, porphyrins, nucleoside phosphates, ATP, vitamins, DNA, and drugs. Ambrogi et al. are noted for intercalating ibuprofen to study the drug release profiles of LDH and are among the first to consider LDH as a passive drug delivery system (Ambrogi et al.). Choy et al. have determined LDH to be a successful non-viral drug and gene delivery vector due to its extensive properties (Choy, Kwak, et al.). Various methods are used to intercalate the negatively charged anions (Kwak et al.; Choy, Kwak, et al.; Khan and O'Hare). The dimensions and functional groups of the guest molecule are important in determining the interlayer spacing within the LDH. The number, size, orientation of the guest molecule, and host-guest interaction, are also critical factors affecting intercalation.

Homogeneously nucleated intercalated LDH nanoparticles have also been studied for *in vitro* and *in vivo* applications. The LDH is an ideal platform for drug delivery as it gives a great deal of stability to the intercalated species and can be synthesized from divalent and trivalent ions (Mg^{2+}, Zn^{2+}, Fe^{3+}, Al^{3+}) which, in small concentrations, have little to no toxicity in biological environments. Along

with the species above, LDH has been intercalated with therapeutic agents such as ketoprofen (Silion et al.), plasmid DNA (pDNA) (Ladewig et al.), Indomethacin (Del Arco et al.), and podophyllotoxin (Qin et al.), as well as dyes such as Lucifer Yellow and fluorescein isothiocyanate (Flesken-Nikitin et al.). Such studies have reported the overall toxicity of LDH and on the efficacy of the intercalated species.

It is well know that any pharmaceutical drug within a biological system can have unwanted side effects. Ibuprofen, for example, can cause severe lesions when applied in high doses. M Silion et al. completed an *in vivo* study on ketoprofen intercalated LDH with the hopes of revealing the gastrointestinal effects of pure ketoprofen and how these are mitigated when combined with LDH. As expected, pure ketoprofen caused gastrointestinal ulcerations. However, when intercalated into (Zn, Al) or (Mg, Al) LDH, the ulcerations were minimized, and in some cases, completely eliminated (Silion et al.). Other studies have shown similar effects with Indomethacin intercalated LDH. Again, when treated with pure Indomethacin, the test subjects experienced severe stomach ulcerations, however the size and severity of the lesions were greatly reduced when the drug was incorporated into the LDH structure (Del Arco et al.).

Through the above discussion, an overall trend can be seen. Most notably, the need for improved treatment options with minimal unwanted side effects has turned the attention to nanomedicine. Decades of research have been put into nanomedicine leading to the development of polymeric, quantum dot, LDH, and core-shell platforms for biological applications with one primary goal: improvement of diagnostic and/or therapeutic capabilities while minimizing cytotoxicity. The use of quantum dots for bioimaging has drastically improved

the fluorescent yield (when compared to available biomolecules) while simultaneously all but eliminating the issue of high toxicity common to many fluorescent biomolecules. Core-shell systems have combined various materials to produce nanoparticle platforms with enhanced properties. A thin silica shell, for example, is commonly used to improve the absorption properties of noble metal core while also providing a biocompatible surface for the attachment of fluorescing biomolecules. Finally, and most interestingly, LDH has been successfully intercalated with various therapeutic drugs and organic dyes. By incorporating these species into the LDH structure, overall stability is improved and the unwanted side effects reduced. *In vivo* studies on intercalated LDH have provided proof of the beneficial properties of such a system.

Although there has been significant progress with nanomedicine in recent years, further improvement is always warranted and necessary. Using past successes as an outline, novel nanomedicinal platforms may be developed. As example, a gold-core/LDH-shell nanoparticle system may prove to be an ideal platform for a multi modal theranostic. Reported studies on the beneficial properties of a nanoparticle gold core (Bardhan, Grady and Halas; Chance, Prock and Silbey) and intercalated LDH (Ambrogi et al.; Silion et al.; Del Arco et al.) give promise to the success of the described Au-core/LDH-shell system. The successful development of such a system may prove to be the basis for next generation nanomedicine and open the doorway for the exciting developments to come.

CHAPTER 3

EXPERIMENTAL

Chemicals

3-aminopropyl-trimethoxysilane (APTMS, 97%), aluminum nitrate nonahydrate ($Al(NO_3)_3 \cdot 9H_2O$, 98+%), citric acid (99.5%), fluorescein isothiocyanate (FTIC), gold(III) chloride hydrate ($HAuCl_4 \cdot xH_2O$, >49% as Au), iron(III) nitrate nonahydrate ($Fe(NO_3)_3 \cdot 9H_2O$, 99.99+%), magnesium nitrate hexahydrate ($Mg(NO_3)_2 \cdot 6H_2O$, 99%), NaOH (min. 98%), NH_4OH (27% aqueous solution), sodium silica solution (~10.6% Na_2O, ~25.6% SiO_2), and trisodium citrate dihydrate (Na-cit, 99%) were all purchased from Sigma Aldrich, and used as received without any further purification. Barnstead Nanopure deionized water with resistivity up to 18MΩ·cm was used for all synthesis procedures.

Preparation of Materials

Preparation of Gold NPs & Surface Functionalization with Silica Coating

Au NPs were prepared using a well documented method (Mine et al.; Lee, Yoo and Han); (Lee, Yoo and Han). Initially, 200 ml aqueous solution of 0.24 mM $HAuCl_4$ was prepared. Next, 0.94 ml aqueous solution of 0.34 M trisodium citrate dihydrate (Na-cit) was added and allowed to stir at 80 °C for one hour. At this point, the solution turned a crimson red, indicating the formation of the gold NPs. The solution was allowed to cool and then stored for future use.

The stability of the gold NPs is excellent under synthesized conditions. However, in basic and/or salty experimental media, the aggregation of the Au NPs is rapid, rendering the gold useless. In order to prevent this, it was necessary to coat the gold NPs with a thin shell of silica. Freshly prepared 0.25 ml of 1 mM APTMS was added to 50 ml of the synthesized gold NPs. This

solution was vigorously stirred for five minutes and then allowed to stand for an additional 30 minutes. Next, one part $NaSiO_3$ (10.69%) was diluted 20 times with nanopure water. Then, 2 ml of the diluted $NaSiO_3$ solution was added to gold nanoparticle/APTMS solution and stirred vigorously for 10 minutes. The solution was then allowed to stand for at least 24 hours.

Synthesis of Au-Core/LDH-Shell

A solution with Mg^{2+} : Al^{3+} as the respective divalent and trivalent ions (3 : 1 ratio, respectively) was prepared. Here, 0.3846 g [$Mg(NO_3)_2 \cdot 6H_2O$] and 0.1876 g [$Al(NO_3)_3 \cdot 9H_2O$] were added into a 500 ml volumetric flask and then filled to 500 ml with H_2O and mixed thoroughly. The solution was then stored for future use. A second solution containing Mg^{2+} : Fe^{3+} (3 : 1.3 ratio, respectively) was prepared in a 250 ml volumetric flask. Both 0.1923 g [$Mg(NO_3)_2 \cdot 6H_2O$] and 0.1313 g [$Fe(NO_3)_3 \cdot 9H_2O$] were added and then filled to 250 ml H_2O and thoroughly mixed. This solution was used within 30 minutes of preparation and any excess was properly disposed. The two solutions were used as the precursors for LDH synthesis. In the procedure which follows, either solution was used depending on which LDH composition was desired, i.e. (Mg, Al) or (Mg, Fe) LDH.

The LDH was heterogeneously deposited on the prepared gold NPs under high supersaturation conditions. Initially, 2.0 ml gold NPs and 17.0 ml H_2O were mixed in a 250 ml beaker. Under vigorous stirring, 1.0 ml of 100 mM NaOH was then added and stirred for 2 minutes to ensure complete mixing. Finally, 5.0 ml of either metallic salt solution was added, and the solution was stirred for 10 minutes. The suspension was then centrifuged at 7000 rpm for 10 minutes, the

supernatant was removed, and the excess of the salts were eliminated by washing twice with 25 ml nanopure water.

After analyzing the results from the above method, small modifications were made and the procedure was adapted to include polyethylene glycol (PEG). First, 0.001g PEG was added to 40 ml nanopure water and allowed to stir moderately for five minutes. Stirring was maintained at a slow enough speed to prevent the formation of bubbles on the surface of solution. Next, 4.0 ml gold NPs were added to the solution followed by the addition of 2.0 ml 100 mM NaOH. Finally, 5.0 ml of either metallic salt solution was added, and the solution was stirred for 10 minutes. The suspension was then centrifuged at 7000 rpm for 10 minutes, the supernatant was removed, and the excess of the salts were eliminated by washing twice with 25 ml nanopure water.

Intercalation of Au-Core/LDH Shell NPs

Intercalation was completed via two separate processes: during precipitation of the Au-Core/LDH shell NPs and post synthesis direct anion exchange. In order to intercalate during precipitation, a FITC dye solution was first prepared. Here, 1.945 mg FITC was added to a solution of 94.75 ml H_2O and 5.25ml 1M NaOH, producing a 2.0 mM FITC solution. Next, 2 ml of the dye solution was added to 20 ml H_2O and 2.0 ml of the silica functionalized gold NPs and allowed to stir for 2 minutes. After mixing was complete, 0.5 ml of 100 mM NaOH was added followed by 3.0 ml of Mg^{2+}/Al^{3+} salt solution (3 mM Mg^{2+}, 3:1 Mg^{2+}/Al^{3+}). This solution was stirred vigorously at room temperature for 10 minutes. The suspension was then centrifuged at 7000 rpm and washed twice to eliminate the excess of salts and dye.

The direct anion exchange method takes place after the LDH synthesis is complete. A 40 ml suspension of the Au-core/LDH shell was reacted with 0.03g of FITC at 60°C under vigorous stirring for 1 hour. The sample was then centrifuged and washed, while a part of it was dried for PXRD measurements, the rest was resuspended in 40 ml NANOPure water.

Characterization of Au and Au-Core/LDH-Shell Nanoparticles

The Au NPs and Au-core/LDH shell NPs were characterized by dynamic light scattering (DLS), powder X-ray diffraction (PXRD), transmission electron microscopy (TEM), energy dispersive X-ray spectroscopy (EDX), and UV-Vis spectroscopy (UV-Vis). The DLS method was used mainly to determine the particle size and size distribution of both Au NPs and Au-core/LDH shell NPs. The crystallinity of both synthesized Au core and Au-core/LDH shell was determined by PXRD measurements.

The intercalation of dye into Au-core/LDH shell NPs was characterized by the peak position shift in PXRD spectroscopy due to the change of spacing between the LDH layers. Also, Fourier transform infrared spectroscopy (FTIR), and inductively coupled plasma emission (ICPE) was used to detect the presence of dye in the LDH after the intercalation.

CHAPTER 4

RESULTS AND DISCUSSION

Synthesis and Characterization of Au-Core/LDH-Shell Nanoparticles (NPs)

Au NPs and Silica Functionalized Au-Nanoparticle Core

According to DLS measurements, the as synthesized Au NPs have a diameter ~15 nm ± 4 nm. In the as synthesized condition, they are citrate stabilized, and were found to be stable for months, and relatively stable in moderate pH ranges (5.5 - 8.5). However, under LDH precipitation conditions, the presence of the metallic salt strips the citrate molecule from the surface of the gold. Due to a major affinity of chelation between LDH metals and citrate anions, aggregation results almost immediately. Indeed, the DLS results show an increase in size from roughly 15 nm in the citrate stabilized condition to nearly 400 nm once the LDH salt solutions have been added. The same is true with the addition of NaOH to the citrate stabilized gold. As the pH is increased to 11 for example, facilitating the formation of LDH, the solution changes from a crimson red to a light blue almost immediately, again indicating the loss of stability of Au NPs as the ionic strength increases. This change in color can be attributed to the agglomeration of the Au NPs and is described by Rayleigh scattering theory. As the particle size increases, the shorter blue wavelengths are more strongly scattered than red wavelengths and the suspension takes on the light blue color.

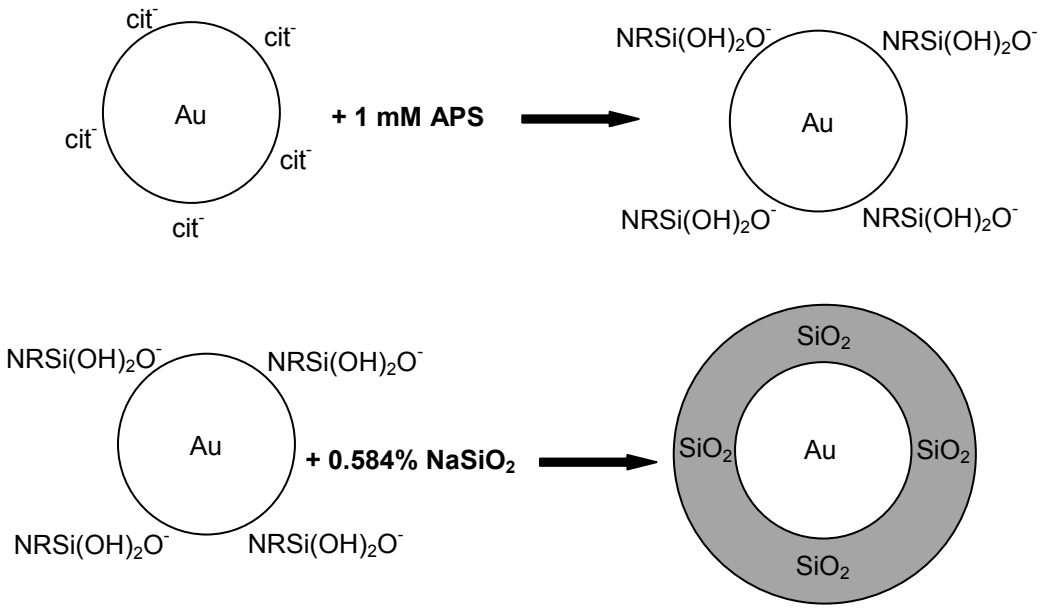

Figure 4 - Schematic diagram of process used to coat Au nanoparticles with thin SiO_2 shell

The primary function of the silica coating is to provide stability to the gold NPs under LDH precipitation conditions. A few reported studies use the Stober method for direct coating of silica onto the Au NPs in alcohol solvent (Mine et al.); (Lu et al.). However, it was found that 12 nm Au NPs agglomerate quickly in alcohol solvent or alcohol/aqueous solvent, and the viability of such a method strongly depends on the initial Au nanoparticle size. The method used here is similar to the one reported by Liz-Marzan (1996) (Liz-Marzan, Giersig and Mulvaney), and a schematic may be seen in Figure 4. It is believed that one monolayer of APTMS is first allowed to adsorb on to the gold colloid surface, with silanol groups pointing into the solution. Hydrolysis of the surface-bonded siloxane form silane triols occurs within minutes, followed by a slow polymerization of silicate groups by adding active silica at pH around 8.5 (Liz-Marzan, Giersig and Mulvaney; Mine et al.). In this way, a thin layer of silica was

built, and the coated Au NPs had a diameter of approximately 30 nm. Prior to coating the gold with silica, the aggregation of the Au cores was severe. The silica-coated gold NPs were placed in both acidic and basic metallic salt (i.e., LDH precursor) solutions after which DLS measurements were made. In both cases, the average particle size remained unchanged when compared to the as prepared silica-coated Au particles. The color also remains unchanged when subjected to the basic media, providing further proof of the stability of the particles.

Au-Core/LDH Shell Nanoparticles (NPs)

The synthesis of mono-disperse Au-core/LDH shell NPs is highly dependent on the experimental conditions, particularly the pH of the solution. Three primary methods have been extensively studied as viable pathways for the formation of Au-core/LDH-shell NPs, i.e., an increasing pH route and a constant pH route at both high and low supersaturation.

The LDH was heterogeneously deposited on the silica-coated gold NPs under high supersaturation conditions. In order to achieve these conditions, it was necessary to ensure the pH of the reaction was maintained within the adequate precipitation range; for Mg (II), the hydroxides form from pH 9.5 to 12.5, for Al (III) the pH range is from 3.3 to 8, however, at pH 12 and higher, the aluminum hydroxides start to be re-dissolved. Various studies have given particular importance to the prevention of polymerization of $Fe(OH)_3$ (Reichle); (Huang et al.); (Costantino et al.). It has been shown that starting at pH 2.4, until pH ~7, the polymerization and precipitation take place simultaneously, and after pH 7, the precipitation is preferred (Dey and Sistiabudi); (Macdonald and Lide). The rapid polymerization of $Fe(OH)_3$ can deplete the system of Fe^{3+} preventing

the formation of LDH. To prevent this, the pH should be maintained above 9. Although increasing the pH would further increase the degree of supersaturation producing more favorable conditions for LDH formation, the stability of the gold NPs becomes an issue as the pH is increased past 11. Thus, a pH ranging between 9.5 and 10.5 was chosen for the precipitation to favor the formation of LDH over the metallic hydroxides.

The polymerization of $Fe(OH)_3$ was also found to cause significant problems prior to the synthesis of LDH. The as prepared Mg^{2+}/Fe^{3+} precursor solution has a pH of approximately 3, and as a result, the polymerization process occurs rapidly. When the solution is freshly prepared it is pale yellow in color. After approximately 30 minutes however, the solution begins to turn a darker red color, indicating the polymerization of $Fe(OH)_3$. At this point, the solution is no longer suitable for use in LDH synthesis.

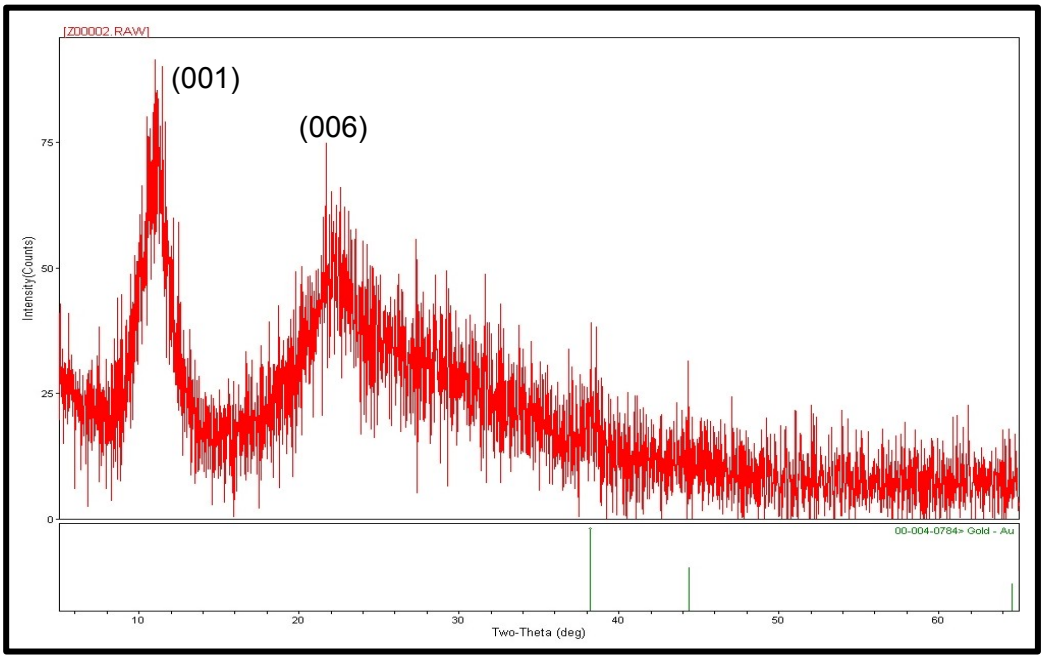

Figure 5 - PXRD Pattern of Au-Core/LDH (Mg^{2+}, Fe^{3+})-Shell

The PXRD technique was used to verify if the LDH structure was obtained; characteristic peaks for a nitrate-intercalated LDH samples should appear at 2-theta angles of roughly 12° and 23°. A small gold peak should also be seen at 38°, however this peak may sometimes be masked if the intensity of the LDH peaks is high or the crystallinity is poor. Figure 5 shows an example of a PXRD pattern obtained from a Au-core/Mg^{2+}/Fe^{3+} LDH shell sample. The characteristic LDH peaks are clearly seen, d_{300} at ~12° implies a gallery spacing around 3.3 Å, which corresponds to the size of nitrate ion. However, the crystallinity is not ideal, which is most likely caused by $Fe(OH)_3$ polymerization. Due to peak broadening, the gold peak is only slightly visible.

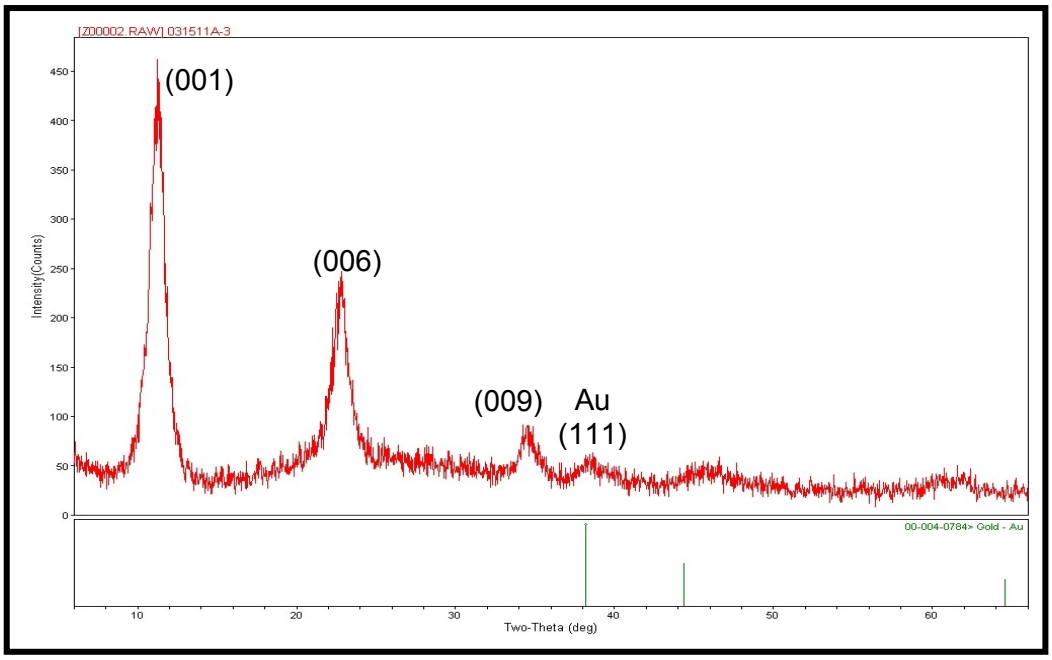

Figure 6 - PXRD pattern of Au-core/LDH-shell NPs in the presence of 0.001g PEG

As indicated in Figure 5, the crystallinity is poor in the original synthesis conditions. Thus, PEG was introduced into the synthesis procedure to help improve the crystallinity of the system and to also improve the stability of the

nanoparticles after synthesis. Figure 6 shows the PXRD pattern obtained from a Au-core/Mg^{2+}/Fe^{3+} LDH shell sample with PEG. The characteristic LDH peaks are again clearly visible, and the intensity of the peaks (and therefore, crystallinity of LDH) is significantly improved when compared to Figure 5. Also notice the small gold peak near 38° which is now visible. The improved crystallinity of the LDH structure reduced the peak broadening and the gold peak is no longer masked. The absorption of PEG onto the surface of the nanoparticles may also provide an additional benefit for future *in vivo* studies. It is believed that PEG also reduces the overall cytotoxicity, allowing for increased doses and elongated release times (Chaves et al.).The DLS technique was used to measure the size of the NPs, and, depending on synthesis conditions, various sizes were obtained. For example, DLS results showed an average effective diameter of 5000 nm for a Au-core/(Mg^{2+}/Fe^{3+}) LDH shell sample, far too large to be reasonably considered for any *in-vivo* application. This led to the investigation of a post-synthesis treatment which would reduce the particle size while still maintaining the desirable properties of LDH. A citric acid treatment was chosen to accomplish this. After measuring the as synthesized particle diameter, 200 µl of 10 mM citric acid was added to the 25 ml sample and the particle size was measured a second time. The sample was then stirred for ten minutes and the particle size was measured again. With no major change between the two measurements, an additional 200 µl of 10 mM citric acid was

Table 1 - Effective diameter before and after citric acid treatment

Volume Citric Acid of 10 mM (µL)	Average Effective Diameter (nm)
0	5056
200	2165
400	1232
400 (after 10 minutes)	115

added and the particle size was measured. Again, the sample was stirred for 10 minutes and the particle size was measured. At this point, the effective diameter was within the desired range and no further treatment was necessary. Table 1 shows the results of one 25ml sample before and after the citric acid treatment. As is seen, the treatment leads to a significant reduction in size, producing particles which are well inside the desired range. However, a comment should be made regarding the economic viability of this process. Although this treatment was found to be both controllable and reproducible, the loss of material is a cause for concern. With such a significant size reduction, a large portion of the LDH components and any intercalated species are lost (approximately 1.0-1.5% loss per 100nm reduction in size). Although the LDH components are relatively inexpensive metallic salts, the loss of which may be acceptable, the intercalated species are generally expensive dyes or chemotherapeutic drugs. The waste of these chemicals would not be economically viable unless retrievable.

Figures 7, 8, and 9 that follow provide a comparison of the DLS results, respectively, from a sample prior to the citric acid treatment, after the citric acid treatment, and a separate sample which was synthesized in the presence of PEG. Three features of these Figures are of importance: effective diameter, polydispersity, and the shape of the correlation function. The DLS results in Figures 7 and 9 correspond, respectively, to the XRD data given above. XRD results are not given for samples after the CA treatment as poor initial crystallinity coupled with particle size effects led to XRD patterns with a single large amorphous hump.

The effective diameter, which includes the actual particle size and any additional hydrodynamic radius (assumed to be negligible), is an average of all

the particles measured throughout the 180 second measurement (~50-100 kilocounts per second). To be applicable for *in vivo* applications, the effective diameter of the completed nanoparticle should be no more than 300nm.

When working with nanoparticles, synthesizing a sample with a uniform particle size is a difficult task. However, a monodisperse suspension is absolutely essential for this, or any, nanoparticle system, as it gives a degree of statistical confidence that minimal large outliers are found in sample (Chan and Nie; Chaves et al.; Mine et al.). The polydispersity is a measure of the particle size uniformity and is simply a ratio between each measured particle size and the overall average. A low polydispersity (0.005-0.250), as seen in Figure 7 and Figure 9, indicates the synthesized nanoparticles are of consistent size.

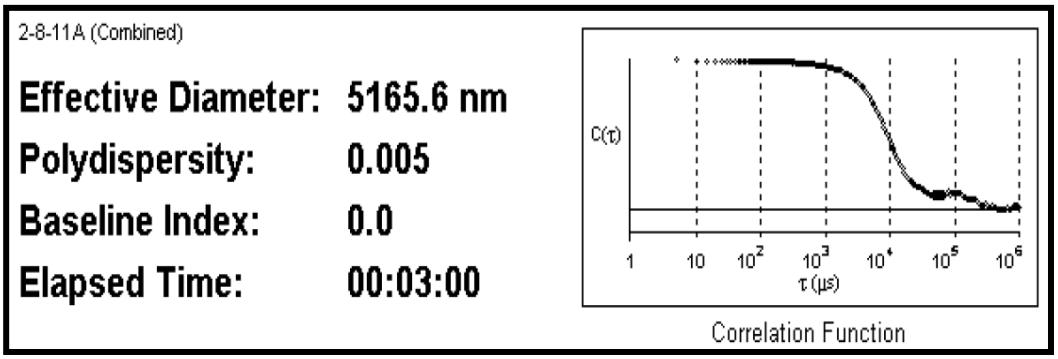

Figure 7 - DLS results summary of Au-core/LDH shell sample prior to citric acid treatment

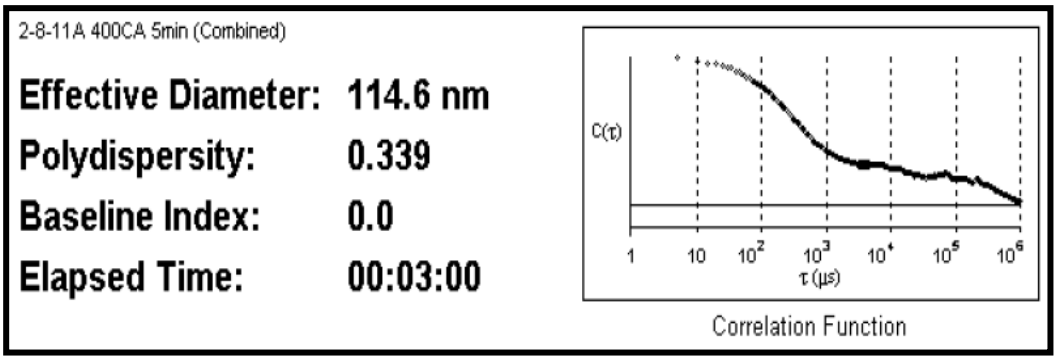

Figure 8 - DLS results summary of Au-core/LDH shell sample after citric acid treatment

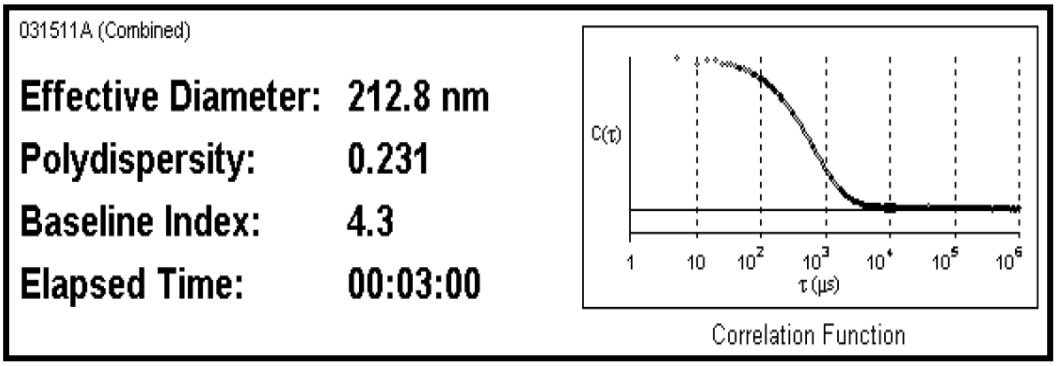

Figure 9 - DLS results summary of Au-core/LDH shell sample synthesized in the presence of PEG

As the polydispersity increases, the system becomes increasingly more like that of large particles outside the desired range. Figure 8, for example, shows a polydispersity of 0.339. Although the effective diameter is only 114 nm,

it is highly likely that a significant number of particles that exceed the desired maximum of 250 nm are present in the sample, which can present problems for *in vitro*/*in vitro* applications.

The shape of the correlation function curve is related to both the size and polydispersity of the nanoparticles. In essence, the correlation function is a measure of how quickly a particle changes position due to Brownian motion. A value at or near 1.0 indicates the particle did not change position in the specified time frame. The sharp decay in the function represents the point at which position of the measure nanoparticle has changed significantly. The smaller the particle, the more quickly it is affected and the decay is seen at a lower time interval. The rate of decay is also related to the polydispersity of the sample. A monodisperse sample will have uniform second order decay, as seen in Figure 7 and Figure 9. As the polydispersity increases, however, size variation throughout the sample becomes significant, and the curve takes on a less regular shape, which is the case in Figure 8.

As Figures 8 and 9 represent the results of completed Au-core/LDH shell samples, a brief comparison is necessary. In both samples, particles within the desired size range were synthesized. The most notable (and significant) lie in the polydispersity and correlation function. The correlation curve of the sample in Figure 8 begins a second order decay near the same time interval as that of the Figure 9 sample, however the decay is extended over a large interval and is very irregular in shape. This is a result of the large polydispersity (0.339) as a result of the citric acid treatment. Although the average particle size could be regularly controlled with the treatment, surfaces of the original particles may be dissolved at various rates and as a result, the shape of the resulting nanoparticles was

unpredictable leading to a larger polydispersity index. The correlation curve seen in Figure 9 however, maintains a second order decay until a near zero value is reached. A quick comparison with the samples corresponding polydispersity index shows a value within the desired range (0.231). Through this analysis, it was easy to determine that PEG provided a much more thorough and reasonable solution to both the size and stability of nanoparticle suspensions.

It is worthy to mention that so far, no literature has shown the direct synthesis of a Au-core/LDH-shell nanoparticle system. One group has reported a Fe_3O_4-core/(Mg,Al) LDH shell system synthesized through the physical adsorption of commercial LDH nanosheets on the Fe_3O_4 core (500nm) (Li et al.). The other related study reports synthesis of micron sized $MgFe_{1.03}O_{2.54}$-core/(Mg,Al) LDH shell particles followed by a ball milling process to reduce the particle size (Zhang et al.).

Intercalation of Anionic Dye into LDH Structure

A key benefit of the LDH class of materials is the ability to be intercalated with anionic species such as dyes or therapeutic drugs. Once inside, the LDH structure provides stability to the molecules until they have reached the target site via endocytosis. Once within the cell, the hydroxide layers can be removed by dissolving in the acidic media of the lysosome. This allows the anionic species to be released, thus minimizing any unwanted effects to surrounding areas. In order to test the intercalation capabilities of LDH, the synthesized metallic-core/LDH shell NPs were intercalated with Fluorescein Isothiocyanate (FITC). Finally, the *in vitro* study of the uptake capability of such metallic-core/LDH shell NPs with FITC intercalated by living PC3-PSMA human prostate cancer cells was carried out using fluorescence microscopy.

Figures 10 (a) and (b) show fluorescence microscopy images of the PC3-PSMA cells which have been treated with FITC intercalated (Mg^{2+}, Fe^{3+}) LDH nanoparticles with and without the fluorescence filter, respectively. The obvious fluorescence of the cells may be a result of either a simple staining of the exterior surface or the uptake of the NPs by the cells.

A majority of the cells in the image appear to be lysed. The exact reason is yet to be determined, however, it is assumed that it is a result of toxicity either due to LDH and/or the FITC. The suspension with which the cells were treated contained a small amount of FITC not contained within the LDH structure which may have contributed to the cell death. LD_{50} measurements with LDH will reveal the precise levels at which LDH becomes toxic. From these measurements, the *in vitro* experiments can be modified and improved to provide better results.

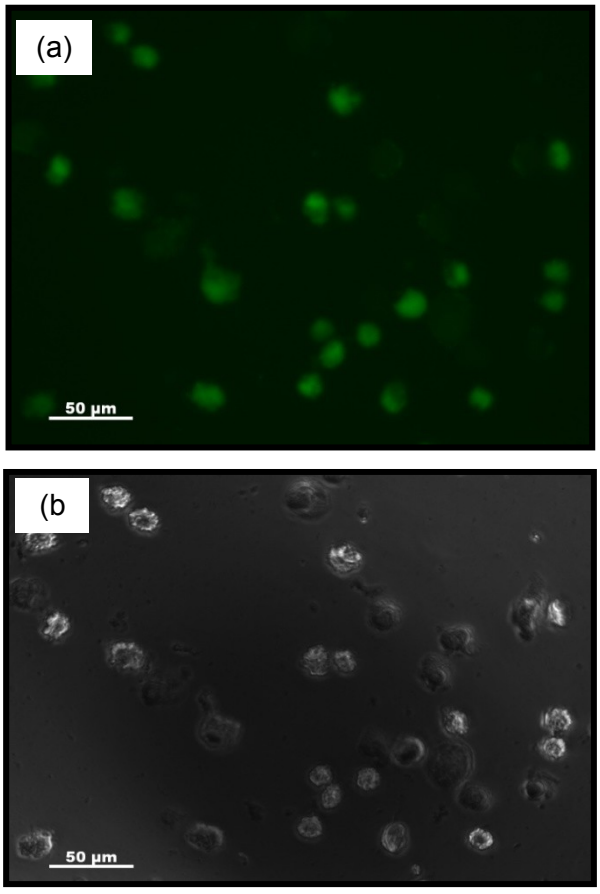

Figure 10 - Fluorescence microscopy images showing the presence of FITC in the cancer cell culture with (a) and without (b) filter

Future PXRD measurements are expected to reveal a shift in the intercalated LDH peaks when compared to those prior to intercalation. In the as synthesized condition without intercalation, the gallery between LDH layers

consists of water and CO_3^{2-}/NO_3^- anions. When intercalated, these species are replaced with the intercalating agent. Because the two species have a different size, the gallery spacing must change accordingly, and the corresponding peak shift will be seen on the PXRD pattern. Fourier transform infra-red spectroscopy (FTIR) will also show the presence of FITC in the interlayer spacing of the LDH; spectra of pre- and post-intercalation samples should look the same except for the vibrations corresponding to the dye, which is expected to be present in the post-intercalation samples.

CHAPTER 5

CONCLUSIONS AND FUTURE WORK

Au-core-LDH (Mg^{2+}, Fe^{3+}, or Al^{3+}) shell nanoparticles for the potential therapeutic and diagnostic treatment of cancer cells have been synthesized and characterized. The primary therapeutic functions include hyperthermic ablation by NIR absorption and apoptosis induced by anionic therapeutics (conjugated Adriamycin or siRNA).

The development of this Au-core/LDH shell platform has led to the successful synthesis of a stable silica-coated gold nanoparticle cores, overcoming the severe aggregation of the citrate-stabilized gold core under LDH deposition conditions. The LDH shell was heterogeneously deposited on the silica/gold core, however the as synthesized size (~3μm) was found to be far too large for *in vitro* and *in vivo* applications. As a result, a post synthesis citric acid treatment was developed, which enables a controlled size reduction to the desired diameter (~200nm). The PXRD pattern showed broad, low intensity peaks, which is a result of the poor crystallinity of the LDH shell. Also, the absence of several diffraction peaks indicated that the shell is composed of only a few LDH sheets, inferring the preferred growth in the horizontal direction.

Although the citric acid treatment had moderate success, particularly in short term stabilization of the suspension, a large portion of material was lost, and the overall crystallinity of the LDH shell was poor. To circumvent this issue, PEG was used during the initial stages of synthesis. The PXRD of the core-shell with PEG revealed a much higher crystallinity and the stability of the suspensions remained as good if not better than samples treated with citric acid. The most significant benefit from the use of PEG, however, was the direct synthesis of

nanoparticles with the desired size. Moreover, with PEG, it was no longer necessary to dissolve the outer layers of the LDH shell, which would have led to significant waste. Finally, since countless works have reported using PEG to further functionalize the surface of various nanoparticles, the Au-core/LDH-shell with PEG may be used in the future to functionalize the surface of the nanoparticles with site specific targeting ligands for cancer treatment.

Future work will first focus on completing the characterization of the intercalated LDH system as described above. Substantial *in vitro* testing is required to obtain more conclusive results pertaining to the uptake of the core/shell nanoparticles. The final steps will involve the surface functionalization, which could improve the uptake efficacy (with site specificity) by cancer cells, and demonstration of the multimodality of this theranostic system.

An interesting property of the gold nanoparticle core which must be further investigated is the surface plasmon resonance (SPR). This unique property causes a strong absorption at a specific frequency, around 520nm for gold NPs although the exact position is strongly dependent on both size and shape (aspect ratio) of the nanoparticles (Liz-Marzan, Giersig and Mulvaney). The strong absorption causes a significant increase in temperature. This characteristic can be exploited for hyperthermal ablation. By fine tuning the structure and geometry of the Au-core/LDH shell NPs, the SPR can be shifted into near infra-red frequencies (NIR ~800nm), which is much more useful for *in vitro* and *in vivo* applications as organic body tissues do not strongly absorb at NIR frequencies.

REFERENCES

Ambrogi, V., et al. "Intercalation Compounds of Hydrotalcite-Like Anionic Clays with Antiinflammatory Agents - I. Intercalation and in Vitro Release of Ibuprofen." *International Journal of Pharmaceutics* 220.1-2 (2001): 23-32. Print.

Bardhan, R., N. K. Grady, and N. J. Halas. "Nanoscale Control of near-Infrared Fluorescence Enhancement Using Au Nanoshells." *Small* 4.10 (2008): 1716-22. Print.

Boclair, J. W., and P. S. Braterman. "Layered Double Hydroxide Stability. 1. Relative Stabilities of Layered Double Hydroxides and Their Simple Counterparts." *Chemistry of Materials* 11.2 (1999): 298-302. Print.

Brannon-Peppas, L., and J. O. Blanchette. "Nanoparticle and Targeted Systems for Cancer Therapy." *Advanced Drug Delivery Reviews* 56.11 (2004): 1649-59. Print.

Bruchez, M., et al. "Semiconductor Nanocrystals as Fluorescent Biological Labels." *Science* 281.5385 (1998): 2013-16. Print.

Carlino, S. "The Intercalation of Carboxylic Acids into Layered Double Hydroxides: A Critical Evaluation and Review of the Different Methods." *Solid State Ionics* 98.1-2 (1997): 73-84. Print.

Chan, W. C. W., and S. M. Nie. "Quantum Dot Bioconjugates for Ultrasensitive Nonisotopic Detection." *Science* 281.5385 (1998): 2016-18. Print.

Chance, R. R., A. Prock, and R. Silbey. "Lifetime of an Excited Molecule near a Metal Mirror - Energy-Transfer in Eu3+-Silver System." *Journal of Chemical Physics* 60.5 (1974): 2184-85. Print.

Chaves, C. R., et al. "Application of Core-Shell Pegylated Cds/Cd(Oh)(2) Quantum Dots as Biolabels of Trypanosoma Cruzi Parasites." *Applied Surface Science* 255.3 (2008): 728-30. Print.

Choy, J. H., et al. "Layered Double Hydroxide as an Efficient Drug Reservoir for Folate Derivatives." *Biomaterials* 25.15 (2004): 3059-64. Print.

---. "Cellular Uptake Behavior of Gamma-P-32 Labeled Atp-Ldh Nanohybrids." *Journal of Materials Chemistry* 11.6 (2001): 1671-74. Print.

Corporation, Brookhaven Instruments. "Dynamic Light Scattering Theory". Holtsville, 2010. Correlation function example. Brookhaven Instruments Corporation. April 16 2011.

Costantino, U., et al. "New Synthetic Routes to Hydrotalcite-Like Compounds - Characterisation and Properties of the Obtained Materials." *European Journal of Inorganic Chemistry*.10 (1998): 1439-46. Print.

Del Arco, M., et al. "Mg,Al Layered Double Hydroxides with Intercalated Indomethacin: Synthesis, Characterization, and Pharmacological Study." *Journal of Pharmaceutical Sciences* 93.6 (2004): 1649-58. Print.

Dey, S. K., and R. Sistiabudi. "Ceramic Nanovector Based on Layered Double Hydroxide: Attributes, Physiologically Relevant Compositions and Surface Activation." *Materials Research Innovations* 11.3 (2007): 108-17. Print.

Farokhzad, O. C., and R. Langer. "Nanomedicine: Developing Smarter Therapeutic and Diagnostic Modalities." *Advanced Drug Delivery Reviews* 58.14 (2006): 1456-59. Print.

Flesken-Nikitin, A., et al. "Toxicity and Biomedical Imaging of Layered Nanohybrids in the Mouse." *Toxicologic Pathology* 35 (2007): 804-10. Print.

Huang, Huang-Chiao, et al. "Simultaneous Enhancement of Photothermal Stability and Gene Delivery Efficacy of Gold Nanorods Using Polyelectrolytes." *ACS Nano* 3.10 (2009): 2941-52. Print.

Khan, A. I., and D. O'Hare. "Intercalation Chemistry of Layered Double Hydroxides: Recent Developments and Applications." *Journal of Materials Chemistry* 12.11 (2002): 3191-98. Print.

Kwak, S. Y., et al. "Bio-Ldh Nanohybrid for Gene Therapy." *Solid State Ionics* 151.1-4 (2002): 229-34. Print.

Ladewig, K., et al. "Controlled Preparation of Layered Double Hydroxide Nanoparticles and Their Application as Gene Delivery Vehicles." *Applied Clay Science* 48.1-2 (2010): 280-89. Print.

Lee, H. B., Y. M. Yoo, and Y. H. Han. "Characteristic Optical Properties and Synthesis of Gold-Silica Core-Shell Colloids." *Scripta Materialia* 55.12 (2006): 1127-29. Print.

Li, L., et al. "Fe3o4 Core/Layered Double Hydroxide Shell Nanocomposite: Versatile Magnetic Matrix for Anionic Functional Materials." *Angewandte Chemie-International Edition* 48.32 (2009): 5888-92. Print.

Liz-Marzan, Luis M, Michael Giersig, and Paul Mulvaney. *Langmuir*.12 (1996): 4329-35. Print.

Lu, Y., et al. "Synthesis and Self-Assembly of Au@Sio2 Core-Shell Colloids." *Nano Letters* 2.7 (2002): 785-88. Print.

Macdonald, F., and D. R. Lide. "Crc Handbook of Chemistry and Physics: From Paper to Web." *Abstracts of Papers of the American Chemical Society* 225 (2003): 019-CINF. Print.

Meng, Weiqing, et al. "Preparation and Thermal Decomposition of Magnesium Iron(Iii) Layered Double Hydroxide Intercalated by Hexacyanoferrate(Iii) Ions." Journal of Materials Science, 2004. 4655-57. Vol. 39. Print.

Mine, E., et al. "Direct Coating of Gold Nanoparticles with Silica by a Seeded Polymerization Technique." *Journal of Colloid and Interface Science* 264.2 (2003): 385-90. Print.

Moghimi, S. M., and T. Kissel. "Particulate Nanomedicines." *Advanced Drug Delivery Reviews* 58.14 (2006): 1451-55. Print.

Qin, L. L., et al. "The in Vitro and in Vivo Anti-Tumor Effect of Layered Double Hydroxides Nanoparticles as Delivery for Podophyllotoxin." *International Journal of Pharmaceutics* 388.1-2 (2010): 223-30. Print.

Reichle, W. T. "Synthesis of Anionic Clay-Minerals (Mixed Metal-Hydroxides, Hydrotalcite)." *Solid State Ionics* 22.1 (1986): 135-41. Print.

Sato, T., et al. "Synthesis of Hydrotalcite-Like Compounds and Their Physicochemical Properties." *Reactivity of Solids* 5.2-3 (1988): 219-28. Print.

Silion, M., et al. "In Vitro and in Vivo Behavior of Ketoprofen Intercalated into Layered Double Hydroxides." *Journal of Materials Science-Materials in Medicine* 21.11 (2010): 3009-18. Print.

Tronto, J., et al. "Organic Anions of Pharmaceutical Interest Intercalated in Magnesium Aluminum Ldhs by Two Different Methods." *Molecular Crystals and Liquid Crystals* 356 (2001): 227-37. Print.

Tyner, K. M., S. R. Schiffman, and E. P. Giannelis. "Nanobiohybrids as Delivery Vehicles for Camptothecin." *Journal of Controlled Release* 95.3 (2004): 501-14. Print.

Wei, M., et al. "Studies on the Intercalation of Naproxen into Layered Double Hydroxide and Its Thermal Decomposition by in Situ Ft-Ir and in Situ Ht-Xrd." *Journal of Solid State Chemistry* 177.7 (2004): 2534-41. Print.

Zhang, H., et al. "A Novel Core-Shell Structured Magnetic Organic-Inorganic Nanohybrid Involving Drug-Intercalated Layered Double Hydroxides Coated on a Magnesium Ferrite Core for Magnetically Controlled Drug Release." *Journal of Materials Chemistry* 19.19 (2009): 3069-77. Print.